Three-dimensional geologic model of the northern Nevada rift and the Beowawe geothermal system, north-central Nevada

Janet T. Watt*
Jonathan M.G. Glen*
David A. John*
David A. Ponce*
U.S. Geological Survey, 345 Middlefield Road, Menlo Park, California 94025, USA

ABSTRACT

A three-dimensional (3D) geologic model of part of the northern Nevada rift encompassing the Beowawe geothermal system was developed from a series of two-dimensional (2D) geologic and geophysical models. The 3D model was constrained by local geophysical, geologic, and drill-hole information and integrates geologic and tectonic interpretations for the region. It places important geologic constraints on the extent and configuration of the active Beowawe geothermal system. The geologic framework represented in this model facilitates hydrologic modeling of the Beowawe geothermal system and evaluation of fluid flow in faults and adjacent rock units.

Basin depths were determined using an iterative gravity-inversion technique that calculates the thickness of low-density, basin-filling deposits. The remaining subsurface structure was modeled using 2D potential-field modeling software. Crustal cross sections from the 2D models were generalized for use in the 3D model and consist of six stratigraphic layers defined as low-density basin sediments, volcanic rocks, basalt-andesite rocks of the northern Nevada rift, Jurassic and Cretaceous intrusive rocks, and Paleozoic siliceous and carbonate sedimentary rocks of the upper and lower plates of the Roberts Mountains allochthon, respectively. This simplified stratigraphy was combined with mapped surface geology and was extrapolated across the 3D model area. Features along the northern Nevada rift depicted by the model may represent preexisting crustal structures that controlled the locations and character of Tertiary tectonic and magmatic events related to Basin and Range extension and emplacement of the middle Miocene northern Nevada rift. Several of the geologic features represented are important components of the Beowawe geothermal system. Prominent ENE-trending faults (e.g., Malpais fault) that bound the southern edge of Whirlwind Valley, and older NNW-striking faults (e.g., Dunphy Pass and Muleshoe faults) that form major features of the model, are likely important pathways for geothermal fluids and groundwater flow from the Humboldt River, which may recharge the Beowawe system.

Keywords: aeromagnetics, Beowawe geothermal system, gravity, north-central Nevada, northern Nevada rift, 3D geologic model.

INTRODUCTION

To increase understanding of fluid flow and heat and mass transfer in active geothermal systems (or fossil hydrothermal systems), hydrologists require 3D geologic models that extend to depths of 5–10 km or more. Such models are particularly important for systems located at fault intersections. Ideally, they should portray the major geologic features of an area at an appropriate level of detail that is feasible to grid. Drill holes are usually few, shallow, or nonexistent. Consequently, geologists and geophysicists must generate such models by extrapolation from geologic maps, cross sections, and geophysical data. While these models have many uncertainties, they facilitate hypothesis testing and identification of the geologic features that exert the greatest influence on the geothermal system.

The purpose of this paper is to describe the geology and geophysics of a part of the eastern northern Nevada rift (synonymous with the northern Nevada rift of Zoback, 1979; Zoback et al., 1994) that encompasses the Beowawe geothermal system in north-central Nevada (Fig. 1) and the assumptions, extrapolations, and geophysical modeling conducted to generate a 3D geologic model. The 3D model integrates regional geologic and tectonic interpretations with local geologic, drill-hole, gravity, and magnetic data, and other geophysical information. It is part of a larger effort to increase understanding of fluid flow and ore formation in fossil hydrothermal systems in the Great Basin, such as those that formed Miocene low sulfidation Au-Ag deposits and Eocene Carlin-type gold deposits. The hydrologic parameters of rock units and insights gained from hydrogeologic models of active geothermal systems are being used to develop analogous models for fossil hydrothermal systems (Person et al., 2005).

REGIONAL AND LOCAL GEOLOGY AND RESOURCES

This area of north-central Nevada in the Great Basin has been the focus of various geologic, mineral resource, and geothermal studies (Hofstra and Wallace, 2006 and references therein). The geotectonic evolution of the area is summarized by Dickinson (2006). Major geologic components include thrust sheets of Paleozoic siliciclastic and carbonate rocks of the Antler orogenic belt, Mezozoic to Paleogene granitoid intrusions, Eocene and Oligocene volcanic rocks, and Neogene bimodal dikes, volcanic rocks, and basin fill—all of which are dissected by two sets of Neogene normal faults.

*jwatt@usgs.gov; jglen@usgs.gov; djohn@usgs.gov; ponce@usgs.gov

Geosphere; December 2007; v. 3; no. 6; p. 667–682; doi: 10.1130/GES00100.1; 6 figures; 1 table.

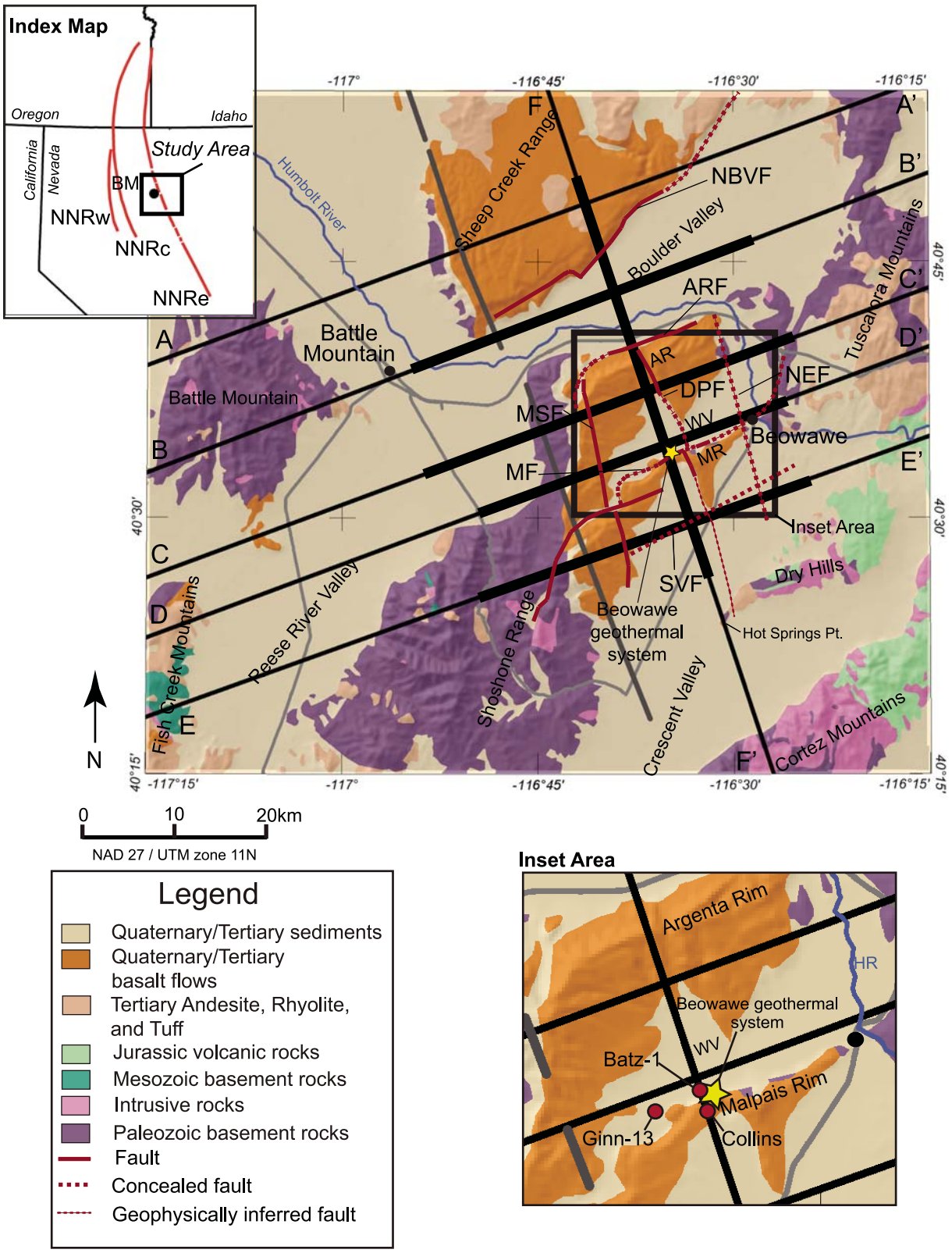

Figure 1. Simplified geologic map of the study area (modified from Stewart and Carlson, 1978) showing the location of the Beowawe geothermal system. Gray lines—roads; red circles—wells; thick black lines—geologic cross-sections; thick dark-gray lines—eastern northern Nevada rift segments; thin black lines—geophysical cross sections A–F; thin red lines on index map—segments of the western, central, and eastern northern Nevada rifts (NNRw, NNRc, and NNRe). AR—Argenta Rim; WV—Whirlwind Valley; MR—Malpais Rim; HR—Humboldt River; BM—Battle Mountain; NBVF—northern Boulder Valley fault; ARF—Argenta Rim fault; MF—Malpais fault; SVF—Southern Valley fault; MSF—Muleshoe fault; DPF—Dunphy Pass fault; NEF—eastern fault. Note that the only faults shown on this figure and the following figures are those that are part of the 3D model.

The discovery of numerous gold-silver deposits, including those along the Battle Mountain-Eureka mineral trend (Roberts, 1966) and the Carlin trend (Roberts, 1960) led to many geologic and geophysical studies focusing on the origin and distribution of these deposits (Berger and Bagby, 1991; Christensen, 1995; Hildenbrand et al., 2000; Grauch et al., 2003). Glen and Ponce (2002) describe several large-scale, NNW-trending, arcuate, mid-Miocene crustal structures in northern Nevada, including the eastern northern Nevada rift, which passes just west of the Beowawe geothermal system and is the focus of this study. The eastern northern Nevada rift has been divided into multiple segments from north to south based on interpretationof magnetic data (Zoback et al., 1994; John et al., 2000; Ponce and Glen, 2008). Zoback and Thompson (1978) and Glen and Ponce (2002) speculate the eastern northern Nevada rift and other associated rifts were localized along regional crustal fractures that were reactivated during emergence of the Yellowstone hotspot along the Oregon-Idaho border.

Previous studies have shown that some epithermal gold deposits are associated with the mid-Miocene intrusive rocks of the eastern northern Nevada rift (Wallace and John, 1998; John and Wallace, 2000; John et al., 2003). Ponce and Glen (2002) used proximity analysis to show that mid-Miocene and younger epithermal gold deposits are both temporally and spatially associated with a number of NNW-trending arcuate crustal features in northern Nevada, including the eastern northern Nevada rift. Large-scale crustal features, such as the eastern northern Nevada rift, may have served as conduits for hydrothermal fluids that formed epithermal gold and other precious metal deposits. Faulted boundaries of such prominent crustal features represent zones of weakness that are commonly reactivated during periods of deformation, often providing pathways for deeply circulating fluids. Accordingly, the faults associated with the eastern northern Nevada rift are likely important to the plumbing of geothermal systems.

The Beowawe geothermal system, located 10 km west of Beowawe in Whirlwind Valley, is a hot-water system that is localized within an area of structural complexity (Christensen, 1980; White, 1992). Trace-element geochemical analyses of drill cuttings suggest fluid flow is restricted to fault zones and permeable horizons (Christensen, 1980). The geothermal system is mainly fault controlled, with the Malpais fault acting as the main flow-controlling structure near the surface (Fig. 1) (Zoback, 1979; Layman, 1984). Struhsacker (1980) and Smith (1983) suggest NNW-trending faults, such as the Dunphy Pass fault, may also be important components of the geothermal system. The older, NNW-trending Dunphy Pass fault zone formed during Miocene east-northeast to west-southwest, rift-related extension, whereas the ENE-trending Malpais fault zone formed after a change in plate motions (10–6 Ma) rotated the extension direction to a northwest-southeast orientation (Zoback and Thompson, 1978; Struhsacker, 1980; Zoback et al., 1981; Wallace and John, 1998). This change in extension direction resulted in the formation of ENE-oriented grabens. The Beowawe geothermal field is located in one of these ENE-oriented grabens that is bounded on the west by the NNW-trending, east-dipping Muleshoe fault (John et al., 2000) and on the east by the NNW-trending, west-dipping Dunphy Pass fault (Struhsacker, 1980). The Malpais fault and related Corral Canyon fault (John and Wrucke, 2003), hereafter referred to as the Malpais faults, form the southern boundary of this ENE-trending graben. Many of the ENE-trending faults, including the Argenta Rim and Malpais faults (Fig. 1), show evidence of left-lateral oblique-slip displacement that offset the eastern northern Nevada rift and associated NNW-trending structures by up to 3 km (Zoback, 1979; John and Wrucke, 2003). The Malpais, Muleshoe, and Dunphy Pass faults are all thought to cut through both upper-plate siliceous rocks and the lower-plate carbonate rocks of the Roberts Mountains thrust.

Based on pore-water chemistry (Sanders and Miles, 1974) and isotopic analyses (John et al., 2003) of the Beowawe geothermal fluids, the deep-source reservoir for the Beowawe geothermal system is thought to be within carbonate rocks of the lower plate of the Roberts Mountains thrust. There may also be intermediate and shallow reservoirs in the upper-plate Valmy Formation and Miocene lava flows, respectively (Struhsacker, 1980). Although the recharge for the deep geothermal system remains largely unresolved, the possible sources include percolation of surface groundwater downward through fractures and normal faults (Struhsacker, 1980; Olmstead and Rush, 1987), flow along either the Dunphy Pass or Malpais faults from their intersections with the Humboldt River, or flow within the fractured Paleozoic siliceous rocks that intersect the Humboldt River valley (Struhsacker, 1980). In addition, Struhsacker (1980) proposed that hot fluid may migrate northward from great depths in Crescent Valley along the southward extension of the Dunphy Pass fault.

METHODS

Gravity and Magnetics

Gravity data for the study were derived from the statewide gravity compilation of Nevada (Ponce, 1997). All data were reduced using standard methods (Blakely, 1995) to isostatic anomalies that emphasize features in the mid- to upper crust by removing long-wavelength variations in the gravity field related to topography (Fig. 2A) (Simpson et al., 1986). In addition, the isostatic gravity data were filtered to remove short-wavelength anomalies presumably associated with shallow features (Fig. 2B). The data were upward continued to 1 km, which involves calculating the gravity field as if the gravity survey were carried out 1 km above the land surface. Both the isostatic and filtered data were gridded at 1 km.

The thickness of Cenozoic basin deposits, or depth-to-basement, was calculated using a modified version (B. Chuchel, 2005, oral commun.,) of an iterative gravity inversion method (Jachens and Moring, 1990) that allows for the inclusion of independent constraints, such as drill-hole and other geophysical data. The inversion process separates the isostatic gravity field into two components—a component generated by the pre-Cenozoic basement and a component produced by the Cenozoic alluvial fill and volcanic deposits. The depth-to-basement estimate is partly based on the density contrast between the dense pre-Cenozoic basement rocks and the less dense alluvial fill and volcanic rocks. The spatial distribution of alluvium, volcanic rocks, and basement was obtained from the 1:500,000-scale geologic map of Nevada (Stewart and Carlson, 1978). The density of basement rocks is allowed to vary horizontally, while the density of Cenozoic deposits varies according to a density-depth function. The density-depth function used in this study is the same as that used for the entire state of Nevada (Jachens and Moring, 1990). In addition, the inversion was constrained with limited drill-hole information and other geophysical data. The regional density-depth function used to calculate the depth-to-basement for the study area may not be appropriate for detailed individual basin analysis, especially where volcanic rocks make up a significant portion of the basin fill, as is the case for many of the valleys in the study area. The depth-to-basement was modified as necessary within individual basins along 2D model profiles where the regional basement surface was unconstrained and geologic or drill-hole information suggested otherwise. Depth-to-basement estimates based on the inversion of gravity data are not exact. Because of the limitations

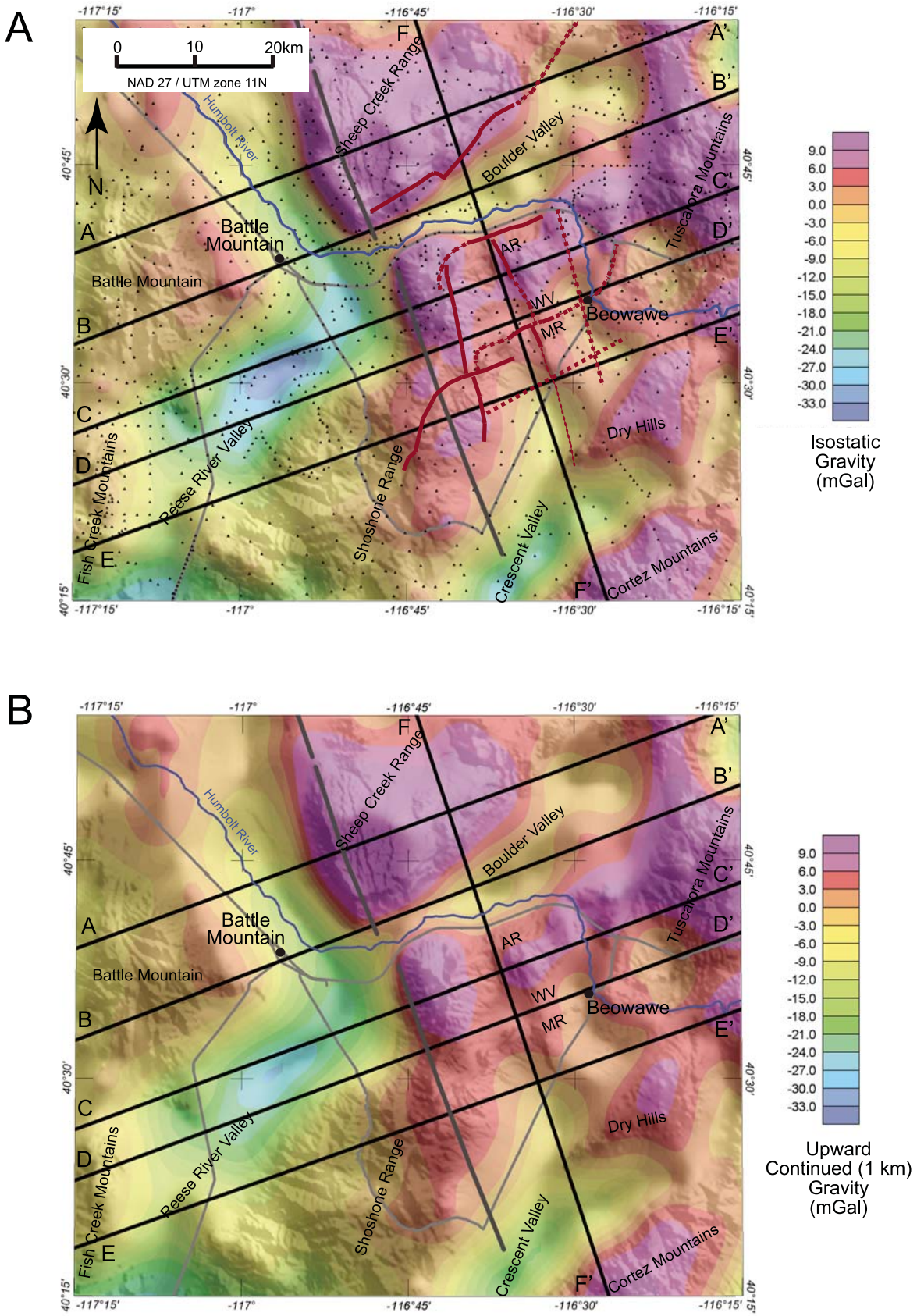

Figure 2. (A) Isostatic gravity map of the study area draped on regional shaded topography. Black triangles—gravity station locations; thick gray line—main trace of western, central, and eastern northern Nevada rifts. (B) Upward continued gravity map showing long-wavelength anomalies. Refer to Figure 1 explanation.

of the regional depth-to-basement process and the inherent ambiguity in the gravity method, on average, estimates are good to within 20%; however, in some cases estimates can be off by 50% in areas of poor gravity data coverage or in areas with thick volcanic deposits.

A residual, total-intensity aeromagnetic map (Fig. 3A) was compiled from a statewide compilation of Nevada (Kucks et al., 2006). Aeromagnetic surveys were flown at different altitudes and with different flight-line spacings, resulting in variable data coverage and resolution. Individual surveys were either upward or downward continued to a common flight-line elevation of 305 m (1000 ft) above the ground, adjusted to a common datum, and merged to produce a uniform map for interpretation. Because a majority of the aeromagnetic surveys were flown at high altitude and coarse flight-line spacing, the resulting maps may not resolve magnetic sources at shallow depths, and caution should be exercised when interpreting short-wavelength anomalies that cross survey boundaries. The poor resolution of the majority of the aeromagnetic data also make it difficult to distinguish between short-wavelength, presumably shallow volcanic rocks and long-wavelength, presumably deep intrusive rocks. In an attempt to separate out shallow and deep sources, the aeromagnetic data were upward continued to 1 km (Fig. 3B). Both the residual and filtered aeromagnetic data were gridded at 1 km.

2D Geophysical Models

A series of 2D geophysical models, in which geologic cross sections were used as the basis for modeling gravity and magnetic data, were created as a foundation for 3D modeling. The 2D models incorporated geologic, gravity, magnetic, and drill-hole information along six profiles covering the study area (Fig. 1). Profiles AA' through EE' trend ENE, perpendicular to the eastern northern Nevada rift, while profile FF' trends NNW, sub-parallel to the rift, and directly through Whirlwind Valley and the active Beowawe geothermal system. Profile FF' was the only profile that was modeled in 2¾-D, which means off-axis bodies were incorporated in the modeling. Because this profile is subparallel to the trend of the eastern northern Nevada rift, off-axis bodies contribute significantly to the observed anomalies. All models extend to 10-km depth below sea level. Profiles DD' and FF' cross Whirlwind Valley and incorporate drill-hole information from the Batz-1, GINN-13, and Collins wells (Fig. 1).

The 2D geophysical modeling strategy for this project requires all model bodies have consistent density and magnetic susceptibility values (Table 1). Rock properties were assigned to geologic units based on average densities and magnetic susceptibilities defined by Carmichael (1982), Johnson and Olhoeft (1984), and Glen et al. (2007, written commun.). The rock properties for the eastern northern Nevada rift and related units were based on the work of Zoback (1979). This approach limits the ambiguity and nonuniqueness of the models by using both regional and local rock property information to assign consistent density and magnetic susceptibility values rather than varying the rock properties to fit the geophysical data. Where misfits in the data occur, we discuss geologic and geophysical scenarios that satisfy the existing data.

Before any geophysical modeling was done, detailed geologic cross sections were constructed for each profile, except for profile AA', focusing on the areas in and around Whirlwind Valley, but not covering the full extent of each profile (thick black lines, Fig. 1). Modeling at the outer edges of the profiles was usually done using only gravity and magnetic data because of limited reliable subsurface geologic information in these areas. The 2D model parameters, including magnetic field strength, magnetic inclination, magnetic declination, and geologic strike were set to 53,800 nT, 65º, 16.5º, and 90º, respectively.

Thirty-one geologic units were modeled, representing thirteen generalized 2D model layers with differing densities based on depth and different remanent magnetizations (see Table 1). The thirteen generalized model layers, represented by unique colors in the 2D models, include mid-crustal rocks, Paleozoic lower-plate carbonate rocks, Paleozoic upper-plate siliceous rocks (including the Roberts Mountains allochthon, Golconda allochthon, Harmony Formation, and an overlap assemblage), Jurassic and Tertiary intrusive rocks, Miocene basalt dikes of the eastern northern Nevada rift, basement rocks containing a significant amount of eastern northern Nevada rift–related Miocene dikes, Jurassic and Tertiary volcanic rocks, Tertiary basalt, and Quaternary and Tertiary alluvium. Model blocks were assigned densities, magnetic susceptibilities, and magnetic remanences according to the predefined values in Table 1. Zoback et al. (1994) estimated that the zone of intrusion is approximately one-third basaltic dikes, based on the magnitude of the gravity anomaly associated with the rift. Rock properties used in our 2D models are consistent with this approximation.

There are a number of ambiguities associated with the 2D geophysical models that need to be addressed. The models themselves are nonunique, in that there are a number of geometries of bodies and physical properties that will fit the observed data. We have tried to limit this uncertainty by incorporating other geologic and drill-hole information where available. Therefore, the 2D models are most constrained where geologic cross sections were available to provide information on the subsurface (Fig. 1). Otherwise, interpretations were based on gravity and magnetic data only. The extents of the eastern northern Nevada rift, related dike units, and intrusive bodies were extrapolated into the subsurface using outcrop locations and predefined lateral extents of these units based on interpretation of regional aeromagnetic and gravity data (Grauch et al., 1988; Grauch, 1996). Where data misfits occurred, the model blocks were altered, making sure the changes were geologically permissible. Where mismatches remained, geophysical data and local geologic information are discussed.

3D Model

A 3D geologic model was created using EarthVision® software. The thirteen generalized layers represented in the 2D geophysical models were simplified to six layers for the 3D model (Table 1). The six layers of the model consist of Paleozoic lower-plate carbonate rocks, Paleozoic upper-plate siliceous rocks, Jurassic and Tertiary granitic intrusive rocks, Miocene basalt dikes of the eastern northern Nevada rift, Tertiary volcanic rocks, and Tertiary and Quaternary alluvium. The eastern northern Nevada rift layer combines both the rift and other Miocene dike units from the 2D modeling. In addition, all Jurassic and Tertiary intrusive units from the 2D modeling are represented by the intrusive layer in the 3D model. Finally, the Paleozoic lower-plate carbonate rock layer in the 3D model includes the mid-crustal unit from the 2D models. Topographic, depth-to-basement, and 2D geophysical model data were integrated to create the six-layer, 3D geologic model of the eastern northern Nevada rift and the Beowawe geothermal system.

Faults deemed important to the formation of the eastern northern Nevada rift or critical to the plumbing system of the Beowawe geothermal system, including the Malpais, Dunphy Pass, Argenta Rim, northern Boulder Valley, eastern northern Nevada rift bounded on eastern side, and south valley faults, were built into the 3D model. Horizon and fault surfaces from the above-mentioned data sets were modeled in EarthVision® and edited until we were satisfied that the model adequately reflected the observed data.

Surfaces from the 2D geophysical models were combined with existing topographic, volcanic, and basement grids to give priority to the

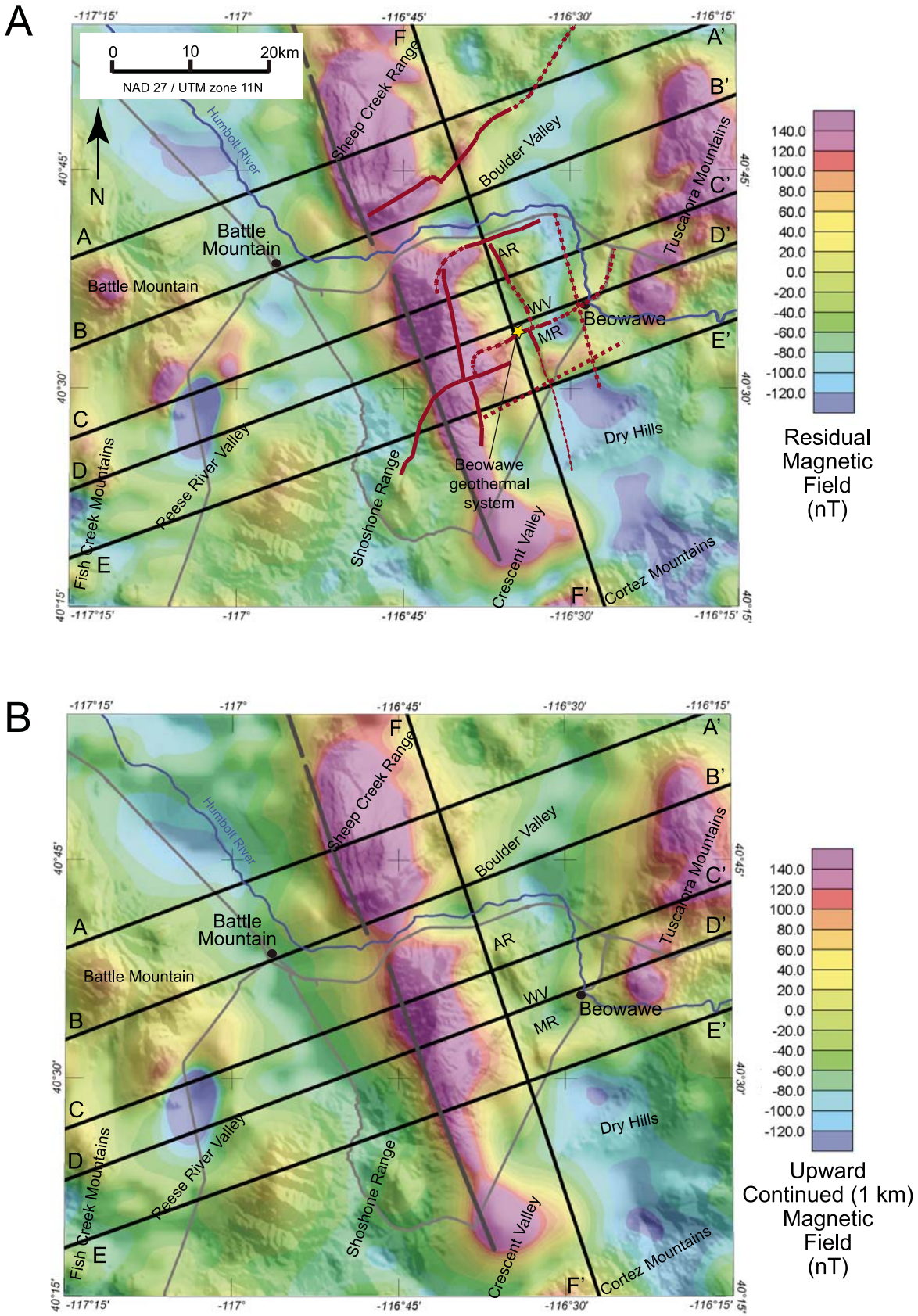

Figure 3. (A) Residual aeromagnetic anomaly map for the study area draped on regional shaded topography. The prominent northwest-trending anomaly in the center of the map is due to magnetic rocks of the western, central, and eastern northern Nevada rifts and related Miocene dike units. (B) Upward continued magnetic map showing long-wavelength anomalies. Refer to Figure 1 explanation.

TABLE 1. STANDARDIZED ROCK PROPERTIES FOR THE GEOLOGIC UNITS IN THE 2D MODELS

3D Model Unit	2D Model Unit	Unit description	Model density (kg/m^3)	Model susc / rem (SI)
QTs	QTs	Quaternary sediments 0-200 m	2020	0
		Quaternary&Tertiary sediments 200-600 m	2120	0
		Quaternary&Tertiary sediments 600-1200 m	2320	0
		Quaternary&Tertiary sediments >1200 m	2420	0
TJv	Tb	Tertiary basalt	2700	0.025
		Tertiary basalt - reversely magnetized	2700	*0.038
	Tv	Miocene dacitic rocks	2500	0.013
		Tertiary rhyolite	2400	0.013
		Tertiary tuff	2400	0.013
	Jv	Jurassic volcanic rocks	2700	0.013
NNRe	NNRe	NNRe intrusive above 2 km	2700	0.019
		NNRe intrusive 2-5 km	2750	0.031
		NNRe intrusive below 5 km	2800	0.038
	NNRe-related dikes prevalent	Pzu+basalt dikes	2670	0.006
		Pzl+basalt dikes	2720	0.013
		Middle crust + dikes 6-11 km	2770	0.025
TJi	Ei1	Eocene intrusive rocks above 2 km	2670	0.013
		Eocene intrusive rocks 2-5 km	2720	0.016
		Eocene intrusive rocks below 5 km	2750	0.019
	Ei2	Eocene intermediate intrusive rocks above 2 km	2720	0.013
		Eocene intermediate intrusive - 2-5 km	2750	0.019
		Eocene intermediate intrusive below 5 km	2770	0.025
	Ji	Jurassic intrusive rocks - above 2 km	2670	0.006
		Jurassic intrusive rocks - 2-5 km	2720	0.009
		Jurassic intrusive rocks below 5 km	2750	0.013
Pzu	Pzu1	Golconda Allochthon	2650	0
		Lower Paleozoic siliciclastic rocks (upper plate of Roberts Mountains Allochthon)	2650	0
	Pzu2	Upper Paleozoic Overlap assemblage	2670	0
		Harmony Formation (feldspathic sandstone)	2670	0
Pzl	Pzl	Lower Paleozoic cabonate rocks (lower plate of Roberts Mountains allochthon)	2690	0
	MC	Middle crust - 6-11 km	2750	0

Note: Susc—magnetic susceptibility.

*Magnetic remanance: 0.126, –65°, 180° (magnetization [SI], inclination, declination).

2D modeled data. The topographic surface used in the 3D model was derived from 30-m digital elevation models (DEMs) in the study area. DEMs were merged and regridded to 120 m. The pre-Cenozoic basement surface was calculated from the inversion of gravity data as described in the Gravity and Magnetic Methods section. The pre-Cenozoic basement surface is synonymous with the top of the Paleozoic upper-plate model layer.

RESULTS and DISCUSSION

Depth to Pre-Cenozoic Basement

The generalized depth-to-basement map (Fig. 4) shows that basin thickness varies significantly among basins. Reese River Valley is characterized by a broad arcuate basin with depths ranging from <500 m northeast of the town of Battle Mountain and west of the Fish Creek Mountains to 4 km west of the town of Battle Mountain. In contrast, Boulder Valley is very shallow, with basin depths averaging less than 500 m. Basin thicknesses up to 3 km in Whirlwind Valley and northern Crescent Valley reflect locally thick accumulations of volcanic rocks within the graben defined by the Muleshoe and Dunphy Pass faults. The apparent extension of thick basin deposits from Whirlwind Valley into northern Crescent Valley supports the work of Olmsted and Rush (1987), who suggested groundwater from the Beowawe geothermal system flows southeastward into Crescent Valley, as well as eastward into the Humboldt River basin. While northern Crescent Valley is quite shallow, southern Crescent Valley has basin depths greater than 5 km in two distinct subbasins.

The depth-to-basement surface was used as a guide for 2D geophysical modeling. However, the regional depth-to-basement surface in Figure 4 often had to be altered for 2D geophysical modeling within individual basins. For example, the regional depth-to-basement is not constrained very well in southern Boulder Valley. The depths in Figure 4 are too shallow. This is likely partly due to the lack of drill-hole data and the existence of thick volcanic deposits surrounding southern Boulder Valley.

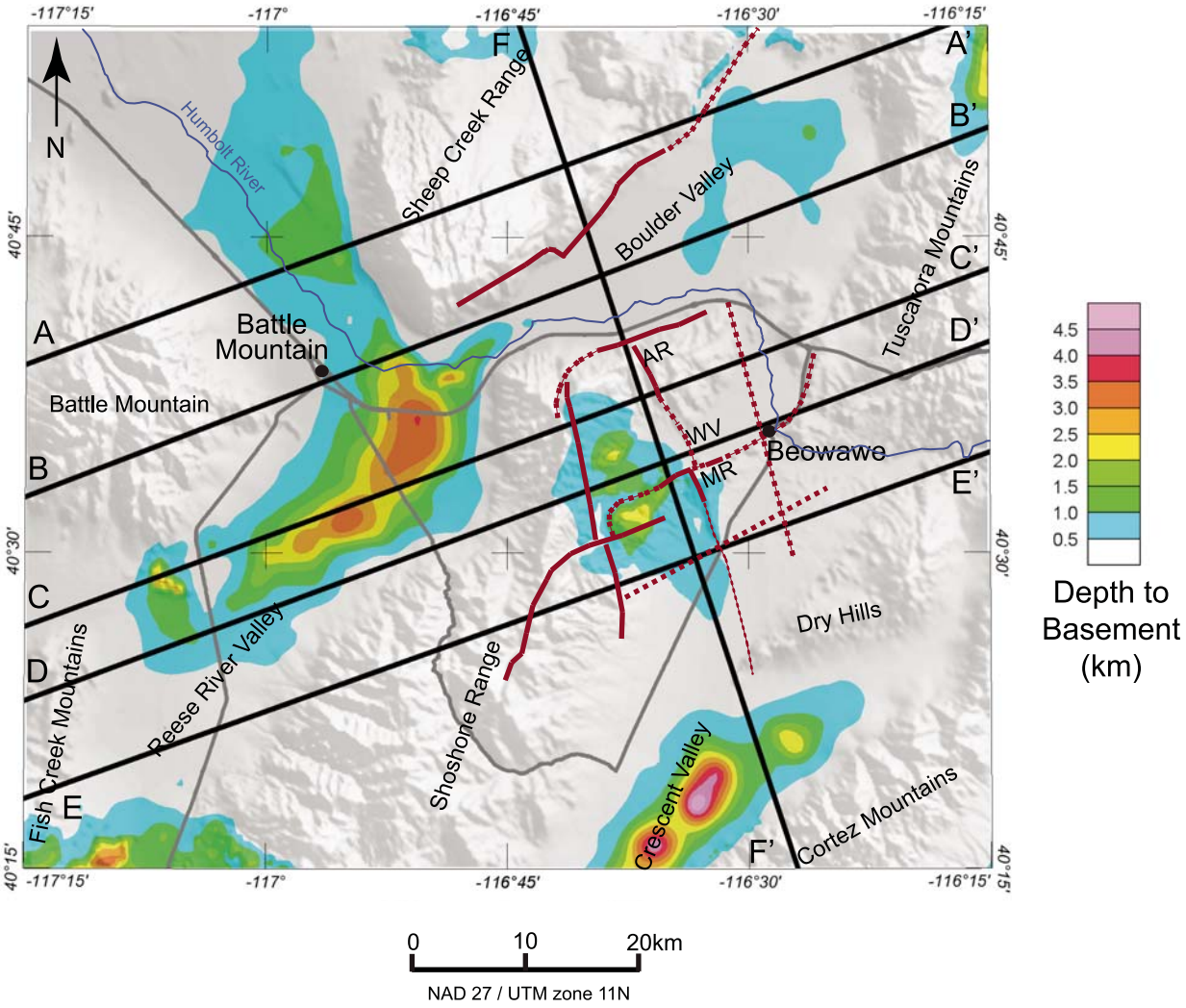

Figure 4. Map showing the depth to pre-Cenozoic basement draped on regional shaded topography. Refer to Figure 1 explanation.

2D Models

The results of the 2D geophysical modeling are presented below, with each profile described in detail, including discussion of important geologic and hydrologic features as well as misfits between the observed and calculated model values (Figs. 5A–5F).

Profile AA'

The northernmost profile, AA', is east-northeast trending and begins at Battle Mountain, crossing northern Reese River Valley and the southern part of the Sheep Creek Range before ending in the southern Tuscarora Mountains along the Carlin trend (Fig. 5A). This profile highlights the asymmetric, half-graben structure of northern Reese River Valley. This part of the valley dips westward, with basin depths up to 2 km along the profile.

The eastern northern Nevada rift is characterized by two distinct zones of Miocene diking, with each zone corresponding to magnetic anomalies 1 and 2 (Fig. 5A). There also appears to be a wide zone of eastern northern Nevada rift–related dikes to the east of anomalies 1 and 2 based on the broad aeromagnetic high visible in the filtered aeromagnetic data (Fig. 3B). In this area, the eastern northern Nevada rift is defined solely by magnetic data, because none of these dike zones are exposed at the surface. The misfits in the magnetic susceptibility are likely due to areas of highly concentrated Miocene dikes in this part of the eastern northern Nevada rift. There is a pronounced gravity gradient, increasing from west to east, at the western edge of the rift. This steep gradient is visible on all profiles to the south, except profile EE', and likely reflects the juxtaposition of dense basement rocks east of the eastern northern Nevada rift, with less dense basin deposits and basement rocks west of the rift (Ponce and Glen, 2008). In profile EE', the gravity gradient is less pronounced because the eastern northern Nevada rift is juxtaposed against dense Paleozoic rocks on the west in the Shoshone Range, which decreases the density contrast.

To the east, this profile crosses the northern Boulder Valley fault, which is a normal fault defining the northern boundary of Boulder Valley. Boulder Valley is very shallow at its northern end (<1 km) along profile AA' (Fig. 4).

Profile BB'

Profile BB' begins in Battle Mountain and crosses Reese River Valley and the eastern northern Nevada rift, which is buried beneath Boulder Valley (Fig. 5B). The profile continues along the axis of Boulder Valley and terminates in the southern Tuscarora Mountains. Similar

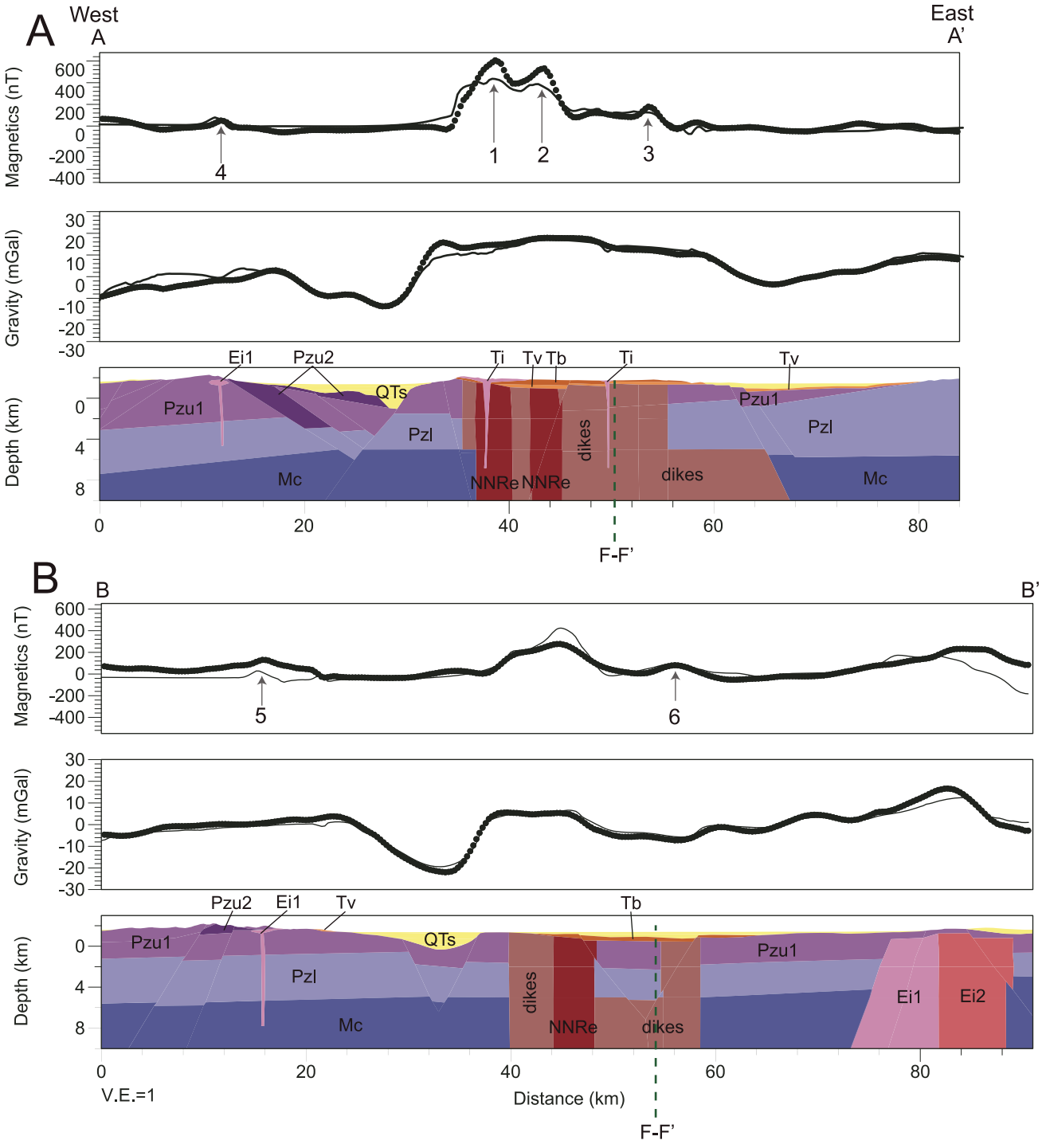

Figure 5A–5F (*continued on next two pages*). Two-dimensional geophysical models along profiles A–F. Profile locations are shown in Figure 1. Dots—observed gravity and magnetic values; green dashed line—crossing profile location; thin black line—calculated (modeled) gravity and magnetic values. Dashed black lines—location of approximate basin axes along profile FF for Boulder and Crescent Valleys. NNRe—eastern northern Nevada rifts.

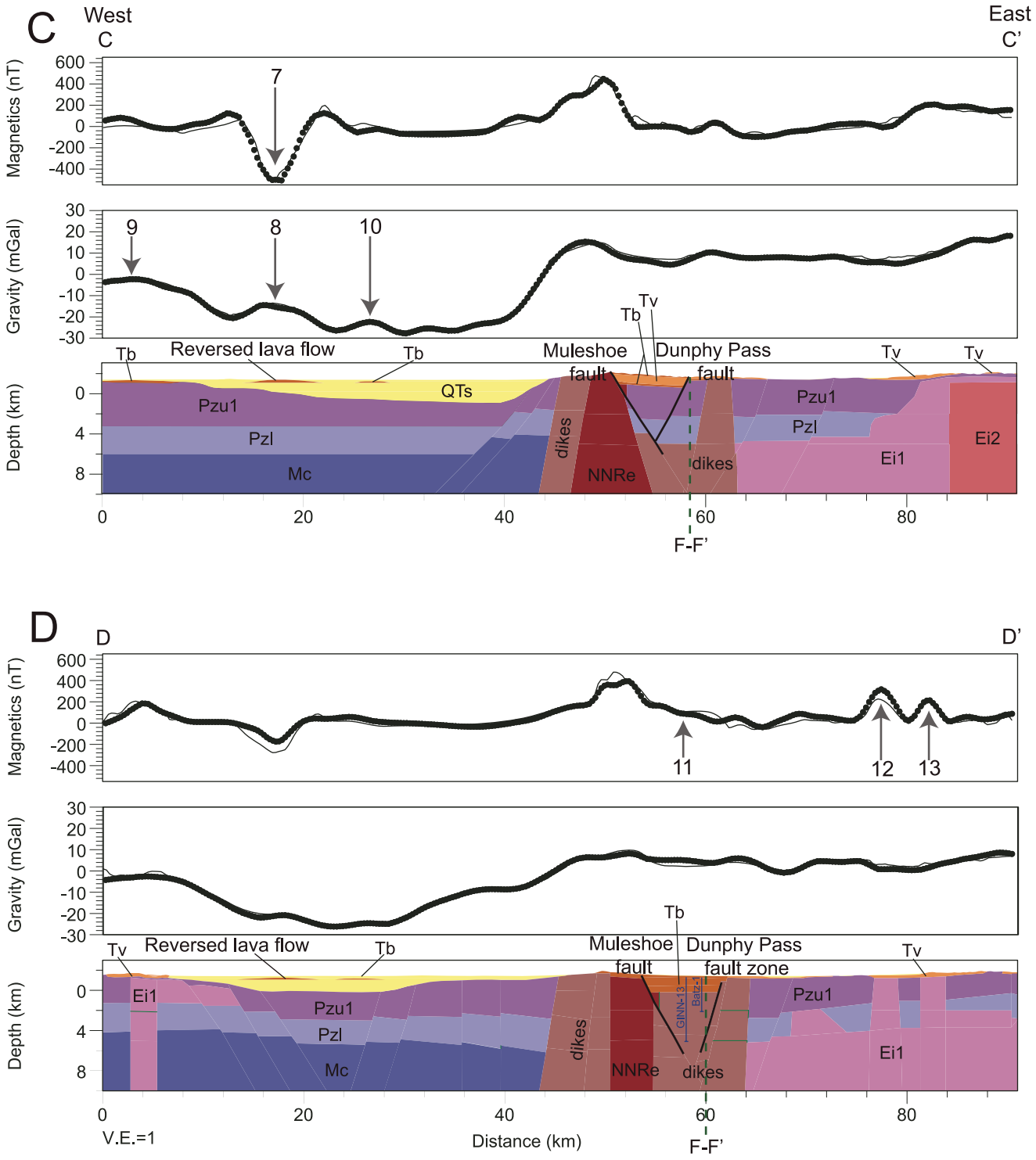

Figure 5 (*continued*).

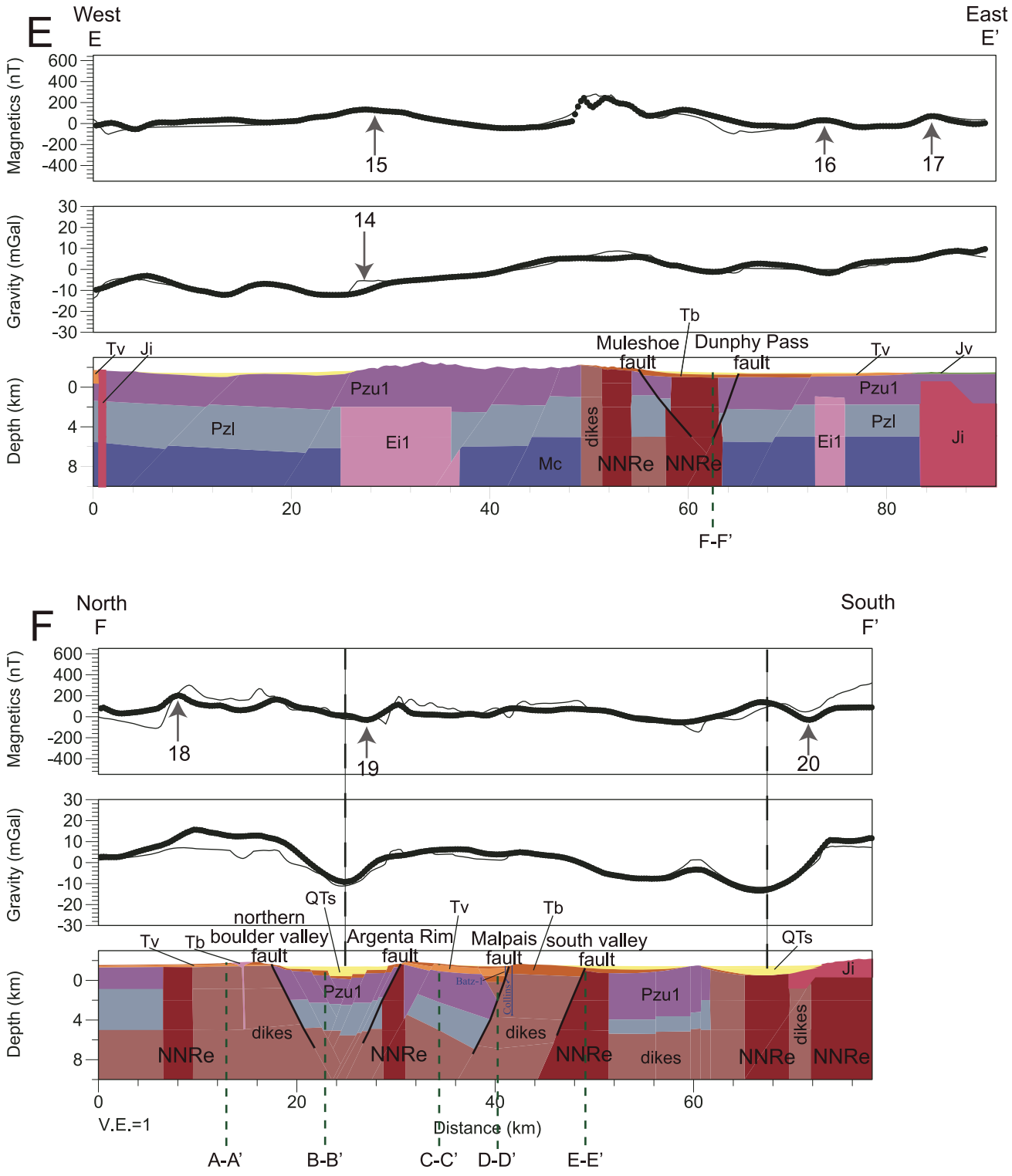

Figure 5 (*continued*).

to profile AA', we modeled a small Tertiary intrusion near the western end of profile BB along the southern margin of Battle Mountain (Fig. 5B, anomaly 5). The large-amplitude gravity low over the Reese River Valley corresponds to a basin thickness of up to 2.5 km along the profile (Fig. 4). The eastern margin of the basin is marked by a steep gravity gradient associated with the western edge of the eastern northern Nevada rift. The eastern northern Nevada rift–related dike complex associated with anomaly 6 in Figure 5B represents what we have interpreted as an eastern splay of the rift. The aeromagnetic high associated with this dike complex along profile BB' is laterally continuous, crossing profiles BB', CC', and DD', and runs parallel to the eastern northern Nevada rift (Figs. 3A and 3B). The misfit between the observed and calculated magnetic values along the eastern northern Nevada rift may be due to the fact that there are fewer dikes in this part of the rift, as suggested by the lack of field evidence for dikes to the north in the southern Sheep Creek Range (John and Wrucke, 2002; Ramelli et al., 2001).

The Muleshoe and the Dunphy Pass faults may extend beneath Boulder Valley, although their presence based on the geophysical data is not definitive. The depth-to-basement map (Fig. 4) suggests southern Boulder Valley is very shallow (<500 m); however, 2D modeling of the geophysical data argues for a slightly deeper basin (up to 1.5 km). On the eastern end of profile BB', we modeled part of the pluton associated with the 38.6 Ma Welches Canyon intrusion (Ressel and Henry, 2006) along the Carlin trend. The misfit in the observed and calculated gravity and magnetic susceptibility models reflects the lack of detailed information on the distribution and rock properties of these intrusive bodies. Improvements to the models may be possible in the future, if new rock property or subsurface mapping data become available.

Profile CC'

Profile CC' begins just south of Battle Mountain and crosses Reese River Valley and the eastern northern Nevada rift before traversing Argenta Rim just north of Whirlwind Valley. Profile CC' continues across a dike complex associated with the eastern northern Nevada rift and terminates in the southern Tuscarora Mountains. We modeled a reversely magnetized volcanic flow along the western part of the profile in Reese River Valley, based on a prominent negative magnetic anomaly and corresponding positive gravity anomaly (Fig. 5C, anomalies 7 and 8) and geologic evidence for ca. 4 Ma basalts to the north along the southern margin of Battle Mountain (Doebrich, 1995). Two other normally magnetized volcanic flows are modeled on either side of this reversed flow, based on positive gravity anomalies 9 and 10 and late Tertiary basalt outcrops in the northern Fish Creek Mountains. These inferred volcanic flows may in fact be rooted by narrow conduits, but we cannot determine whether or not this is the case with existing data.

In profile CC', the eastern northern Nevada rift is cut by the Muleshoe fault. The Dunphy Pass fault cuts through Miocene volcanic rocks at the surface, upper-plate siliceous rocks, and lower-plate carbonate rocks before it is possibly terminated by the Muleshoe fault at a depth of ~5 km.

We infer that the eastern end of profile CC' is underlain by a thick sequence of Eocene intrusive rocks that may be related to the Emigrant Pass volcanic field (Ressel and Henry, 2006) mapped farther north and east. Although these intrusive rocks may not extend all the way west to the eastern northern Nevada rift–related dike complex, the gradual increase in magnetic susceptibility east of the rift-related dikes requires a magnetic body at depth that shallows to the east.

Profile DD'

Profile DD' begins in the northern Fish Creek Mountains and crosses Reese River Valley before clipping part of the Shoshone Range and crossing the eastern northern Nevada rift. Profile DD' then traverses Whirlwind Valley and the Beowawe geothermal area, where the profile runs adjacent to both the deep GINN-13 and Batz-1 geothermal wells (Fig. 1, inset). The GINN-13 and Batz-1 wells were projected onto the geologic cross section for profile DD'. The profile continues eastward over buried eastern northern Nevada rift–related dikes and northern Crescent Valley before ending in the Tuscarora Mountains. The elevated gravity and magnetic values on the western edge of profile DD' (Fig. 5D) and in the filtered gravity and magnetic maps (Figs. 2B and 3B) suggest an intrusive body at depth. Like profile CC', we modeled a reversely magnetized volcanic flow in Reese River Valley; however, this flow appears to be smaller and thinner, suggesting the flow pinches out toward the south. Again, the reversely magnetized flow and adjacent normally magnetized volcanic flows may be rooted by narrow conduits, but we cannot determine this with existing data.

In Whirlwind Valley, the Muleshoe and Dunphy Pass faults define the western and eastern limits of the Beowawe geothermal area. The graben formed by these two faults contains a thick sequence of mostly Miocene volcanic rocks, which are underlain by Paleozoic upper-plate siliceous rocks and lower-plate carbonate rocks. Because the positive magnetic anomaly associated with the eastern northern Nevada rift drops off gradually to the east (Fig. 5D, anomaly 11), rather than sharply as in profile CC', the basement rocks in this area likely have been intruded by Miocene mafic dikes. The Dunphy Pass fault is buried beneath Whirlwind Valley and does not reach the surface. It is unclear whether the Muleshoe and Dunphy Pass faults intersect at depth across this profile. Neither the GINN-13 well nor the Batz-1 well intersects either fault zone.

The eastern end of profile DD' is inferred to be underlain by Eocene plutons associated with the Emigrant Pass volcanic field (Ressel and Henry, 2006), similar in extent to profile CC', but with two apophyses that nearly reach the surface on the far eastern end of the profile. The extents of these apophyses are defined by two distinct magnetic anomalies (Fig. 5D, anomalies 12 and 13). Again, it is speculative that the pluton extends all the way to the eastern northern Nevada rift–related dikes. However, the pluton likely extends westward to the 76-km mark along the profile, based on previous interpretation of aeromagnetic data (Grauch et al., 1988; Grauch, 1996) and geologic investigations by Ressel and Henry (2006).

Profile EE'

Beginning in the Fish Creek Mountains, profile EE' crosses Reese River Valley and the Shoshone Range, before traversing the eastern northern Nevada rift and Crescent Valley. Profile EE' continues eastward into the northern Dry Hills (Fig. 5E). The western end of profile EE' is characterized by a wide alluvial valley underlain by a relatively undissected Paleozoic basement section that is bordered on the west by a Jurassic intrusive body and a thin layer of volcanic tuff in the Fish Creek Mountains. We have extended the intrusive body all the way through the model; however, this is highly speculative. It remains unclear what depth or exactly what shape characterizes this intrusive body.

There is an area in the western Shoshone Range where there is a significant mismatch in the gravity model with the observed gravity values much lower than the calculated values (Fig. 5E, anomaly 14). The sharp gradient in the calculated values reflects the density contrast between valley sediments on the west and mapped basement rocks on the east in the shallow subsurface. To match the observed values, what is needed beneath the mapped basement rocks at the valley margin is a low-density wedge of sediments or rocks, for which there is no geologic evidence. Due to the relatively sparse gravity data in this part of the map (Fig. 2), we conclude that the mismatch may be the result of poor data coverage.

We have modeled a pluton at depth based on the associated long-wavelength magnetic anomaly (Fig. 5E, anomaly 15), the lateral extent of which was previously recognized by Grauch et al. (1988) and Grauch (1996).

In this profile, the Muleshoe and Dunphy Pass faults offset only the dikes related to the eastern northern Nevada rift, and the Dunphy Pass fault does not reach the surface. On its eastern end, profile EE' crosses Crescent Valley where it is shallow (<1 km, Fig. 4). Beneath Crescent Valley and the northern Dry Hills, we modeled two intrusive bodies with different physical properties (Fig. 5E, anomalies 16 and 17). Anomaly 16 is characterized by a gravity low and magnetic high, whereas anomaly 17 corresponds to a gravity high and magnetic low (Figs. 2 and 3). Both of these anomaly patterns appear to be deep seated based on filtered gravity and magnetic data and, therefore, are interpreted as representing intrusive bodies rather than shallow volcanic rocks. Moreover, it is unlikely that anomalies 16 and 17 are related to surficial volcanic deposits. This would require a local thickening of these deposits within a preexisting topographic basin, for which there is not sufficient geologic evidence. Ressel and Henry (2006) suggest there are multiple Eocene plutons feeding the Emigrant Pass volcanic field based on petrographic studies. The geophysical anomaly character of anomaly 16 corresponds to an area in the southern Tuscarora Mountains that may be underlain by Eocene intrusive rocks with a lower density than similar age intrusive rocks to the north and east. The lateral extent of the intrusive body associated with anomaly 17 was previously identified by Grauch et al. (1988) and Grauch (1996), and appears to be associated with the Jurassic intrusive rock mapped in the Dry Hills (Fig. 1).

Profile FF'

Profile FF' runs NNW-SSE, perpendicular to the other profiles. Beginning in the Sheep Creek Range, profile FF' crosses Boulder Valley and Argenta Rim before passing through Whirlwind Valley just west of, and parallel to, the Dunphy Pass fault zone. Profile FF' intersects the Batz-1 and Collins wells in the Beowawe geothermal area before cutting across the Malpais fault and Malpais Rim and dropping into Crescent Valley. The profile continues southward crossing the southern valley fault and Hot Springs Point at the southwestern tip of the Dry Hills before ending in the Cortez Mountains (Fig. 1).

Unlike the other profiles, profile FF' highlights the ENE-trending structures and the north to south complexity of the eastern northern Nevada rift. The Miocene dikes of the eastern northern Nevada rift and related dikes are offset vertically on a number of ENE-trending faults, including the northern Boulder Valley, Argenta Rim, and Malpais faults, which have down-dropped the Miocene dikes to depths between 4 and 7 km within Boulder and Whirlwind Valleys. While not conclusive, there is also evidence of left-lateral offset along these ENE-trending faults (Zoback et al., 1994; John et al., 2000). There are six distinct zones of Miocene diking along profile FF', the northernmost of which is located in the Sheep Creek Range. Basaltic dikes are not exposed at the surface in this area, but the presence of a prominent magnetic anomaly (Figs. 3 and 5F, anomaly 18) suggests there are mafic dikes beneath the surface. The misfit between the observed and calculated gravity values in the Sheep Creek Range may reflect denser basement rocks in this area. The next area of shallow, unexposed Miocene diking is beneath Argenta Rim, and then to the south in northern Crescent Valley, there is a major break in the eastern northern Nevada rift and related dikes that is probably associated with shallow, nonmagnetic Jurassic basement rocks extending west from the Dry Hills (Fig. 3). The southernmost near-surface Miocene dike swarm is located beneath southern Crescent Valley and crops out in the Cortez Mountains southwest of the profile (Gilluly and Masursky, 1965).

If the eastern northern Nevada rift was simply down-dropped within Boulder and southern Crescent Valleys along NNE-trending structures, one would expect the location of the magnetic low to correspond with that of the gravity low. However, in both Boulder and Crescent Valleys, the magnetic low is located at the southern margin of each valley (Fig. 5F, anomalies 19 and 20). Boulder and Crescent Valleys are coincident with left-stepping, segmented magnetic anomalies along the eastern northern Nevada rift (Fig. 1 inset and Fig. 3) identified by Zoback et al. (1994) and John et al. (2000). These segments may reflect offsets along NE-striking, left-lateral faults (e.g., Mabey, 1966; Zoback et al., 1994), or they could reflect primary en echelon emplacement of the eastern northern Nevada rift (Ponce and Glen, 2008).

3D Model

The 3D model presented in this paper provides a simplified, regional geologic framework for future subsurface investigations of this area (Fig. 6A). Inconsistencies within the 3D model arise from heterogeneous data distribution and poorly constrained data. Nonetheless, it is important to mention that the most accurate parts of the model are those where there are either geophysical, geological, or well data to constrain the model. Where there are no data, extrapolations are made by the 3D modeling software using predetermined geologic rules. Some areas of the 3D model are more constrained than others. Specifically, the portion of the 3D model outlined by the black box in Figure 6A has been constrained by geologic mapping, depth to pre-Cenozoic basement estimates, 2D geophysical modeling, and well data and represents the most accurate interpretation. Outside of this box, along the 2D model profiles, the model is constrained by 2D geophysical modeling and depth to pre-Cenozoic basement calculations. The remaining areas of the 3D model are defined by regional depth to basement only, with few constraints on the extent of the eastern northern Nevada rift and intrusive rock bodies. The yellow and blue data points (Fig. 6B) show where the eastern northern Nevada rift and intrusive units, respectively, are constrained.

The faults in this model are all dying faults, meaning their horizontal extents are defined by a polygon window. At the same time, each of the faults cuts through the entire model area vertically, which is likely not the case in reality, but is necessary within the modeling software.

The 3D geologic model of the eastern northern Nevada rift and Beowawe geothermal system offers a unique view of the geologic and potential hydrologic setting of north-central Nevada. The 3D model, showing the complexity of the eastern northern Nevada rift and related structures, provides a baseline for geologic interpretation of the evolution of such large-scale rift structures and possibly highlights areas of future mineral exploration based on the subsurface extents of rift structures and other intrusive bodies. This 3D model also provides insight into the structures and rock units that controlled the extent and configuration of the Beowawe geothermal system.

The surface of the eastern northern Nevada rift appears to undulate from north to south in the study area (Fig. 6B) in response to NNW-directed, rift-related faulting, post-emplacement, ENE-directed faulting, and possibly from preferential magma migration along the rift's segment boundaries. Several unexposed intrusive bodies were modeled in three dimensions in this study (Fig. 6B). Although the 3D geometries of these bodies remain somewhat unresolved because of the difficulty in defining their bottoms, the modeled depths to the tops of these intrusions and their estimated shapes provide important information for hydrologic modelers, because these bodies may be either potential barriers to, or conduits for, subsurface fluid flow based on the degree of fracturing within the unit.

The Beowawe geothermal system is fault controlled, with most investigators agreeing that

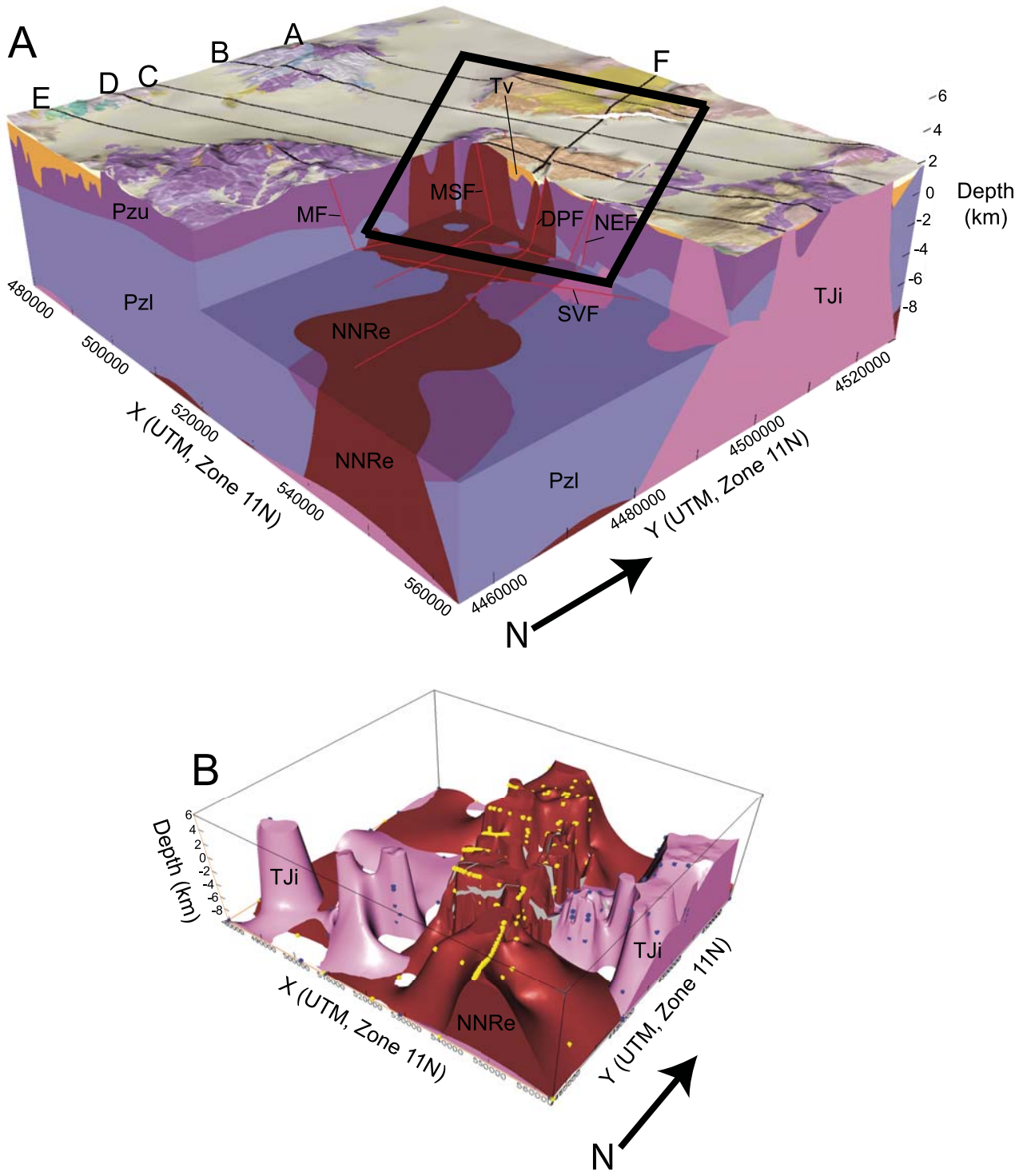

Figure 6. (A) 3D model of the study area, looking northwest along the trace of the eastern northern Nevada rifts (NNRe). Geologic map draped on top of the model was modified after Stewart and Carlson (1978). Thin dashed black lines—profiles A–F; thick black box—model area constrained by geologic mapping, depth to pre-Cenozoic basement estimates, 2D geophysical modeling, and well data. (B) 3D model of only the intrusive rocks (pink) and those of the NNRe (dark red), showing the data points (yellow and blue) from which the surfaces were derived. Vertical exaggeration is 2×.

the intersection of the Malpais and Dunphy Pass fault zones is the main conduit system (e.g., Layman, 1984). The geothermal system is bounded on the west by the east-dipping Muleshoe fault. While the deep reservoir for geothermal fluids is assumed to be the lower-plate Paleozoic carbonates, questions about the geometry and volume of the deep reservoir and the location of recharge areas still remain. The data from the 3D geologic framework model can be used in hydrologic models to test different recharge scenarios to enhance understanding of controls on fluid flow in the deep geothermal system at Beowawe.

CONCLUSIONS

The geology of the eastern northern Nevada rift and the Beowawe geothermal system is complex and is characterized by two distinct sets of structures that play an important role in localizing mineral and geothermal resources and providing conduits for fluid flow—those associated with Miocene east-northeast to west-southwest, rift-related extension, and those resulting from northwest-southeast–directed extension that began between 10 and 6 Ma coincident with a change in Pacific-North American plate motions (Zoback et al., 1981). The 2D models and resulting 3D model of the area illustrate the structural complexity of the eastern northern Nevada rift. Based on our modeling, the eastern northern Nevada rift is a major crustal feature that extends to at least mid-crustal depths. The geometry and geophysical character of previously identified eastern northern Nevada rift segment boundaries in Boulder and Crescent Valleys were further constrained by 2D geophysical modeling and provide a baseline for further studies regarding the formation of the rift and its relationship to Basin and Range tectonics.

The integration of geophysical modeling and detailed geologic information within a 3D model has allowed us to extend knowledge of the shallow subsurface to mid-crustal depths, providing a volumetric framework for hydrologic modeling. The 3D geologic model can be used to estimate deep, geothermal reservoir geometries, identify the relative importance of fault-controlled versus distributed flow, and determine potential recharge pathways for the Beowawe geothermal system. On a more regional scale, the geophysical modeling of gravity and magnetic data identifies and/or constrains the position of buried intrusive bodies. While the exact geometry of these bodies remains unresolved, the modeled depths to the tops of these intrusions and their estimated shapes are important features for hydrologic modeling and exploration for pluton-related ore deposits.

ACKNOWLEDGMENTS

This manuscript was greatly improved thanks to the thorough reviews of Tien Grauch and Thomas Chapin and the constructive comments of associate editor, Al Hofstra.

REFERENCES CITED

Berger, B.R., and Bagby, W.C., 1991, The geology and origin of Carlin-type gold deposits, *in* Foster, R.P., ed., Gold metallogeny and exploration: Glasgow, Blackie and Son, p. 210–248.

Blakely, R.J., 1995, Potential theory in gravity and magnetic applications: New York, Cambridge University Press, 441 p.

Carmichael, R.S., 1982, Magnetic properties of minerals and rocks: Boca Raton, Florida, CRC Press.

Christensen, O.D., 1980, Trace-element geochemistry of gradient hole cuttings: Beowawe geothermal area, Nevada: University of Utah Research Institute Earth Science Laboratory Report no. 48, 28 p.

Christensen, O.D., 1995, The Carlin trend giant gold camp: Is it the strata, the structure or the stocks?, *in* Clark, A.H., ed., Giant ore deposits II—Controls on the scale of orogenic magmatic-hydrothermal mineralization: Kingston, Ontario, Proceedings of the Second Giant Ore Deposits Symposium, 2 April 1995, p. 340–352.

Dickinson, W.R., 2006, Geotectonic evolution of the Great Basin: Geosphere, v. 2, no. 7, p. 353–368, doi: 10.1130/GES00054.1.

Doebrich, J.L., 1995, Geology and mineral deposits of the Antler Peak 7.5-minute quadrangle, Lander County, Nevada: Nevada Bureau of Mines and Geology Bulletin 109, 44 p.

Gilluly, J., and Masursky, H., 1965, Geology of the Cortez quadrangle, Nevada, with a section on gravity and aeromagnetic surveys by D.R. Mabey: U.S. Geological Survey Bulletin 1175, 117 p.

Glen, J.M.G., and Ponce, D.A., 2002, Large-scale fractures related to inception of the Yellowstone hotspot: Geology, v. 30, no. 7, p. 647–650, doi: 10.1130/0091-7613(2002)030<0647:LSFRTI>2.0.CO;2.

Grauch, V.J.S., 1996, Magnetically interpreted, granitoid plutonic bodies in Nevada: Nevada Bureau of Mines and Geology Open-File Report 96-2, chapter 7, p. 7-1–7-16.

Grauch, V.J.S., Blakely, R.J., Blank, H.R., and Oliver, H.W., Plouff, Donald, and Ponce, D.A., 1988, Geophysical delineation of granitic plutons in Nevada: U.S. Geological Survey Open-File Report 88-11, 7 p., 2 plates, scale 1:1,000,000.

Grauch, V.J.S., Rodriguez, B.D., Bankey, V., and Wooden, J.L., 2003, Evidence for a Battle Mountain-Eureka crustal fault zone, north-central Nevada, and its relation to Neoproterozoic-Early Paleozoic continental breakup: Journal of Geophysical Research, v. 108, no. B3, doi: 10.1029/2001JB000681.

Hildenbrand, T.G., Berger, B., Jachens, R.C., and Ludington, S., 2000, Regional crustal structures and their relationship to the distribution of ore deposits in the Western United States, based on magnetic and gravity data: Economic Geology and the Bulletin of the Society of Economic Geologists, v. 95, p. 1583–1603.

Hofstra, A.H., and Wallace, A.R., 2006, Metallogeny of the Great Basin: Crustal evolution, fluid flow, and ore deposits: U.S. Geological Survey Open-File Report 2006-1280, 37 p., http://pubs.usgs.gov/of/2006/1280/.

Jachens, R.C., and Moring, B.C., 1990, Maps of the thickness of Cenozoic deposits and the isostatic residual gravity over basement for Nevada: U.S. Geological Survey Open-File Report 90-404, 15 p.

John, D.A., and Wallace, A.R., 2000, Epithermal gold-silver deposits related to the northern Nevada rift, *in* Cluer, J.K., Price, J.G., Struhsacker, E.M., Hardyman, R.F., and Morris, C.L., eds., Geology and ore deposits 2000: The Great Basin and beyond: Reno, Nevada, Geological Society of Nevada Symposium Proceedings, May 15–18, 2000, p. 155–175.

John, D.A., and Wrucke, C.T., 2002, Geologic map of the Izzenhood Spring quadrangle, Lander County, Nevada: U.S. Geological Survey Miscellaneous Investigations Map I-2668, scale 1:24,000.

John, D.A., and Wrucke, C.T., 2003, Geologic map of the Mule Canyon quadrangle, Lander County, Nevada: Nevada Bureau of Mines and Geology Map 144, scale 1:24,000.

John, D.A., Wallace, A.R., Ponce, D.A., Fleck, R.J., and Conrad, J.E., 2000, New perspectives on the geology and origin of the northern Nevada rift, *in* Cluer, J.K., Price, J.G., Struhsacker, E.M., Hardyman, R.F., and Morris, C.L., eds., Geology and ore deposits 2000: The Great Basin and beyond: Reno, Nevada, Geological Society of Nevada Symposium Proceedings, May 15–18, 2000, p. 127–154.

John, D.A., Hofstra, A.H., Fleck, R.J., Brummer, J.E., and Saderholm, E.C., 2003, Geologic setting and genesis of the Mule Canyon low-sulfidation epithermal gold-silver deposit, north-central Nevada: Economic Geology and the Bulletin of the Society of Economic Geologists, v. 98, p. 425–463.

Johnson, G.R., and Olhoeft, G.R., 1984, Density of rocks and minerals: Boca Raton, Florida, CRC Press.

Kucks, R.P., Hill, P.L., and Ponce, D.A., 2006, Nevada magnetic and gravity maps and data: A website for the distribution of data: U.S. Geological Survey Digital Data Series DS-234, http://pubs.usgs.gov/ds/2006/234/.

Layman, E.B., 1984, A simple basin and range fault model for the Beowawe Geothermal System, Nevada: Geothermal Resources Council, Transactions, v. 8, p. 451–456.

Mabey, D.R., 1966, Regional gravity and magnetic anomalies in part of Eureka County, Nevada, *in* Hanson, D.A., Heinrichs, W.E., Jr., Holmer, R.C., MacDougall, R.E., Rogers, G.R., Sumner, J.S., and Ward, S.H., eds., Mining geophysics: Tulsa, Oklahoma, Society of Exploration Geophysicists, v. 1, p. 77–83.

Olmsted, F.H., and Rush, F.E., 1987, Hydrogeologic reconnaissance of the Beowawe Geysers Geothermal Area, Nevada: Geothermics, v. 16, no. 1, p. 27–46, doi: 10.1016/0375-6505(87)90077-0.

Person, M., Gao, Y., Hofstra, A., John, D., Howard, K., Sweetkind, D., and Prudic, D., 2005, Numeric models of fluid flow in Great Basin geothermal systems and Tertiary hydrothermal gold deposits: Role of high permeabilitiy fault zones: Reno, Nevada, Geological Society of Nevada Symposium 2005, Window to the World, May 14–18 2005, p. 1324–1325.

Ponce, D.A., 1997, Gravity data of Nevada: U.S. Geological Survey Digital Data Series DDS-42, 27 p., CD-ROM.

Ponce, D.A., and Glen, J.M.G., 2002, Relationship of epithermal gold deposits to large scale fractures in northern Nevada: Economic Geology and the Bulletin of the Society of Economic Geologists, v. 97, p. 3–9.

Ponce, D.A., and Glen, J.M.G., 2008, A prominent basement feature along the northern Nevada rift and its geologic implications, north-central Nevada: Geosphere (in press).

Ramelli, A.R., House, P.K., Wrucke, C.T., and John, D.A., 2001, Geologic map of the Stony Point Quadrangle, Lander County, Nevada: Nevada Bureau of Mines and Geology Map 131, scale 1:24,000.

Ressel, M.W., and Henry, C.D., 2006, Igneous geology of the Carlin Trend, Nevada: Development of the Eocene plutonic complex and significance for Carlin-type gold deposits: Economic Geology and the Bulletin of the Society of Economic Geologists, v. 101, p. 347–383.

Roberts, R.J., 1960, Alignments of mineral districts in north-central Nevada: U.S. Geological Survey Professional Paper 400-B, p. B17–B19.

Roberts, R.J., 1966, Metallogenic provinces and mineral belts in Nevada: Sparks, Nevada, American Institute of Mining, Metallurgical, and Petroleum Engineers, Pacific Southwest Mineral Industry Conference, May 5–7, 1965: Nevada Bureau of Mines and Geology Report, v. 13, p. 47–72.

Sanders, J.W., and Miles, M.J., 1974, Mineral content of selected geothermal waters: Reno, University of Nevada, Desert Research Institute, Water Resources Reservoir Project Report 26.

Simpson, R.W., Jachens, R.C., Blakely, R.J., and Saltus, R.W., 1986, A new isostatic residual gravity map of the conterminous United States with a discussion on the significance of isostatic residual gravity anoma-

lies: Journal of Geophysical Research, v. 91, no. B8, p. 8348–8372.
Smith, C., 1983, Thermal hydrology and heat flow of Beowawe geothermal area, Nevada: Geophysics, v. 48, no. 5, p. 618–626, doi: 10.1190/1.1441492.
Stewart, J.H., and Carlson, J.E., 1978, Geologic map of Nevada: Nevada Bureau of Mines and Geology Map, scale 1:500,000.
Struhsacker, E.M., 1980, The geology of the Beowawe geothermal system, Eureka and Lander counties, Nevada: University of Utah Research Institute, Earth Science Laboratory report, no. 37, 78 p.
Wallace, A.R., and John, D.A., 1998, New studies on Tertiary volcanic rocks and mineral deposits, northern Nevada rift-east, *in* Tosdal, R.M., ed., Contributions to the gold metallogeny of northern Nevada: U.S. Geological Survey Open-File Report 1998-338 (CD-ROM), http://pubs.usgs.gov/of/1998/of98-338/chapters/chp22.pdf.
White, D.E., 1992, The Beowawe Geysers, Nevada, before geothermal development: U.S. Geological Survey Bulletin 1998, 25 p.
Zoback, M.L., 1979, A geologic and geophysical investigation of the Beowawe geothermal area, north-central Nevada: Stanford University Publications in the Geological Sciences, v. 16, 79 p.
Zoback, M.L., and Thompson, G.A., 1978, Basin and range rifting in northern Nevada: Clues from a mid-Miocene rift and its subsequent offsets: Geology, v. 6, p. 111–116, doi: 10.1130/0091-7613(1978)6<111:BARRIN>2.0.CO;2.
Zoback, M.L., Anderson, R.E., and Thompson, G.A., 1981, Cenozoic evolution of the state of stress and style of tectonism of the Basin and Range province: Philosophical Transactions of the Royal Society of London, v. A300, p. 407–434, doi: 10.1098/rsta.1981.0073.
Zoback, M.L., McKee, E.H., Blakely, R.J., and Thompson, G.A., 1994, The northern Nevada rift: Regional tectonomagmatic relations and middle Miocene stress direction: Geological Society of America Bulletin, v. 106, p. 371–382, doi: 10.1130/0016-7606(1994)106<0371:TNNRRT>2.3.CO;2.

Manuscript Received 1 March 2007
Revised Manuscript Received 21 August 2007
Manuscript Accepted 25 August 2007